Journal of ELECTRONIC MATERIALS, Vol. 45, No. 6, 2016
DOI: 10.1007/s11664-016-4446-0
© 2016 The Minerals, Metals & Materials Society

CrossMark

The Properties of *p*-GaN with Different Cp_2Mg/Ga Ratios and Their Influence on Conductivity

LIN SHANG,[1,2,4] SHUFANG MA,[1,2] JIAN LIANG,[1,2] TIANBAO LI,[1,2] CHUNYAN YU,[1,2] XUGUANG LIU,[1,3] and BINGSHE XU[1,2,5]

1.—Key Laboratory of Interface Science and Engineering in Advanced Materials, Taiyuan University of Technology, Ministry of Education, Taiyuan 030024, People's Republic of China. 2.—Research Center of Advanced Materials Science and Technology, Taiyuan University of Technology, Taiyuan 030024, People's Republic of China. 3.—College of Chemistry and Chemical Engnineering, Taiyuan University of Technology, Taiyuan 030024, People's Republic of China. 4.—e-mail: shanglin0601@126.com. 5.—e-mail: xubs@tyut.edu.cn

The effect of Cp_2Mg/Ga ratio on the properties of *p*-GaN was explored by scanning Hall probe, photoluminescence (PL), and atomic force microscopy measurement. It was found that *p*-GaN has an optimal doping concentration under 2% Cp_2Mg/Ga ratio, and higher or lower doping concentration is not beneficial to the conductivity. Hole concentration under the optimum condition is 4.2×10^{17} cm^{-3} at room temperature. If the Cp_2Mg/Ga ratio exceeds the optimum value of 2%, surface morphology and electrical conduction properties become poor, and blue emission at 440 nm, considered deep donor-to-acceptor pair transitions in the PL spectra, are dominant. The decrease in electrical properties indicates the existence of compensating donors because the hole concentration decreases at such high Cp_2Mg/Ga ratio. The obtained results indicate that Mg is not incorporated in the exact acceptor site under a heavy doping condition, but acts as a deep donor, instead.

Key words: *p*-GaN, Cp_2Mg/Ga ratio, Mg doping, hole concentration, PL spectra

INTRODUCTION

Mg-doped GaN post-annealing was the solution to realize low resistance *p*-type GaN material, and Shuji Nakamura was awarded a Nobel prize in physics in 2014 for the great discovery. *p*-GaN will supply holes to the active region and recombine with electrons to emit visible blue or green light. The hole concentration and conductivity in *p*-GaN is important to obtain a high efficiency light-emitting diode (LED) device. Thus, further investing the growth parameter on the properties of *p*-GaN is important for us to realize high conductivity *p*-GaN. However, *p*-GaN is difficult to obtain high conductivity owing to high Mg activation energy, reportedly in the range of 120–250 meV,[1–4] the compensation of deep donors, and the limited solubility of Mg in GaN.[5–7] Especially, the compensation phenomenon is very important to determine the conductivity in *p*-GaN. The origin and nature of compensating donors are still controversial, and several donor candidates and mechanisms are considered in the literature.[8–10] Little is known about the Mg doping state at *p*-GaN and its effects on the optical properties of GaN. The effects of Cp_2Mg/Ga ratio or doping concentration on the *p*-GaN grown by metal-organic chemical vapor deposition (MOCVD) have been investigated in the literature.[11–14] However, very few reports have focused on the relationship of its electrical properties with optical properties and surface morphology. It is, therefore, necessary to investigate further the effects of Cp_2Mg/Ga ratio on the properties of *p*-GaN and the relationship between electrical and optical properties.

In this paper, *p*-GaN samples were grown under different Cp_2Mg/Ga ratios in gas phase. The electrical properties such as carrier concentration, mobility, and resistivity were measured with Hall

(Received October 12, 2015; accepted March 1, 2016; published online March 16, 2016)

test. The surface morphology was tested with atomic force microscopy (AFM). The optical properties were analyzed by measuring photoluminescence (PL) spectroscopy.

EXPERIMENTAL

The p-GaN films were grown on sapphire using a $3 \times 2''$ wafer MOCVD (Aixtron TS300) system, with trimethylgallium (TMGa), ammonia (NH_3), and magnesocene (Cp_2Mg) as the metal–organic precursors for Ga, N, and Mg, respectively. A series of 0.5-μm-thick Mg-doped GaN films with different Cp_2Mg/Ga ratios of 1%, 2%, 3%, 4%, and 5% in gas phase were grown on 2-μm-thick undoped GaN with a donor background concentration of 4×10^{16} cm^{-3}. The growth temperature and pressure of the p-GaN films were 960°C and 150 mbar, respectively. The TMGa flow rate was fixed with 21.3 μmol/min and the Cp_2Mg flow rate varied at 0.21 μmol/min, 0.42 μmol/min, 0.63 μmol/min, 0.84 μmol/min, and 1.05 μmol/min, corresponding to Cp_2Mg/Ga ratio of 1%, 2%, 3%, 4%, and 5%, respectively. Afterwards, annealing was carried out in a nitrogen environment at a temperature of 750°C for 15 min to depassivate the Mg-H complexes in the p-GaN thin films.

The electrical and optical properties were measured using Hall (HMS-300) and PL (RMS2000) instruments. The electrical properties were characterized at room temperature by the van der Pauw Hall measurement method using an In electrode for ohmic contacts. The optical properties were measured by PL using a 266 nm wavelength of a pulsed Nd-YAG laser with an excitation density of 17 W/cm^2 as the excitation source. The surface morphology was studied by AFM (SPA-300HV) in tapping mode, and the tip radius curvature was 10 nm. For each wafer, four samples are cut off with 1×1 cm^2 chosen from the center part on the 2-inch wafer to avoid a possible error from the nonuniform growth environment across the entire wafer. At each Cp_2Mg/Ga ratio, two runs with the same Cp_2Mg/Ga ratio were adopted to avoid the run to run variation. The run-to-run variation such as thickness, doping concentration, composition, and growth rate is less than 5%, which ensures the results are exact.

RESULTS AND DISCUSSION

The electrical properties of the samples were characterized at room temperature by Hall measurement. At each Cp_2Mg/Ga ratio, two runs with the same Cp_2Mg/Ga ratio were adopted to avoid run-to-run variation. For test results from different runs, there are no obvious variation, which indicates that the runs were uniform. For each Cp_2Mg/Ga ratio, eight points were tested to calculate carrier concentration and mobility. Figure 2 shows the average carrier concentration and mobility from eight test points of p-GaN as a function of Cp_2Mg/Ga ratio with error bars. It is observed that the hole concentration initially increases with increasing Cp_2Mg/Ga ratio from 1% to 2% in gas phase. When the Cp_2Mg/Ga ratio is larger than 2%, the hole concentration gradually decreases. The doping concentration increases with the increase of Cp_2Mg/Ga ratio in gas phase. This indicates that excess Mg doping is not beneficial to obtain high hole concentration and decreases the hole concentration instead. The reason for the hole concentration decrease at higher Cp_2Mg/Ga ratio will be discussed later. The mobility tends to decrease with Cp_2Mg/Ga ratio. The decrease in mobility at higher doping concentration may originate for two reasons: increased impurity scattering produced by Mg doping and effect of defects induced by Mg doping. The I–V curves of the samples are shown in Fig. 2. The p-GaN sample with 2% Cp_2Mg/Ga ratio has the smallest slope, which indicates the best conductivity. Its resistivity is 1.14 Ω cm, which is the smallest. The conductivity becomes worse as the Cp_2Mg/Ga ratio increases from 2% to 5% (Fig. 1).

The AFM images in Fig. 3 show the surface morphology of p-GaN with different Cp_2Mg/Ga ratio. Striking morphological differences are noticeable. The p-GaN with 2% Cp_2Mg/Ga ratio shows rough surface morphology, as delineated by steps. Hillocks can been observed on the surface. The rough surface means that the epilayer is grown three dimensionally in addition to two-dimensional lateral growth. The surface of p-GaN with 3% Cp_2Mg/Ga ratio is covered with very small grains along with steps. For 5% p-GaN, the grain size further increases, and there is no stepped morphology at the surface. It is known that *in situ* analysis provides reflectivity information such as growth rate during the growth. There are almost no changes in growth rate because there are no obvious variations in the *in situ* curve recorded during different Cp_2Mg/Ga ratio growth. The obvious changes of surface morphology indicate that there

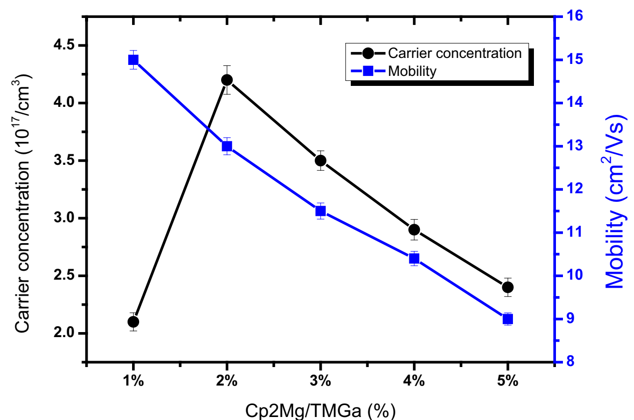

Fig. 1. Average carrier concentration and mobility from eight test points of p-GaN as a function of Cp_2Mg/Ga ratio with error bars.

is a change in growth mode, which originates from high Mg doping concentration. Combined with the Hall test results, it can be concluded that for an excess Cp_2Mg/Ga ratio, the surface exhibits grains for which the size increases with an increase of Cp_2Mg/Ga ratio. Thus, through AFM observation, whether the Cp_2Mg/Ga ratio is excess can be judged by the grain size.

PL study on semiconductors can give us information on the energy level of dopants from the PL spectra and the recombination progress via these energy levels. Thus, in order to study the energy state of Mg dopants at different Cp_2Mg/Ga ratio, PL measurement was carried out to study the optical properties of the series of Mg doped samples. Figure 4 shows the room-temperature PL spectra of the p-GaN with different Cp_2Mg/Ga ratio. The photo-excitation source is a pulsed Nd-YAG laser operating at 266 nm with power density of 17 W cm^{-2}. Three dominant emission peaks at 360 nm, 385 nm, and 440 nm are observed in these samples, which can be resolved by Gaussian fitting. However, the emission bands of these three peaks are quite different. The 1% and 2% Cp_2Mg/Ga ratio samples show only 360 nm and 385 nm bands, and the 2% sample has higher intensity at 385 nm, but lower at 360 nm compared with the 1% sample. The other three samples exhibit nearly quenched 360 nm emission and gradually weakened 385 nm emission at higher Cp_2Mg/Ga ratio. The peak at 360 nm is the near-band-edge emission in GaN and the intensity of this peak weakens gradually with an increase of Cp_2Mg/Ga ratio. The emission band peak at around 385 nm can be observed at lower doping level. The origin of this emission band has been extensively investigated in the literature.[15,16] It is ascribed to the shallow donor–acceptor (D–A) recombination involving isolated Mg substituting the Ga site (Mg_{Ga}) acting as acceptor. The isolated Mg acceptor is in a shallow acceptor state with an activation energy around 200 meV, around 1% of which can be activated after post-annealing. The increase in PL intensity at the 385 nm peak through the increase of Cp_2Mg/Ga ratio from 1% to 2% indicates that the incorporated Mg is in a shallow acceptor state. More Mg in the shallow acceptor state with an increase of Cp_2Mg/Ga ratio will supply more holes in p-GaN. When the Cp_2Mg/Ga ratio is 3%, 440 nm emission corresponding to 2.8 eV appears. From Fig. 4, it is apparent that the 440 nm emission peak becomes gradually dominant, and the 385 nm emission peak is gradually quenched as Cp_2Mg/Ga ratio increases from 3% to 5%. This emission peak was previously reported for highly Mg-doped GaN and attributed to a nearest-neighbor association of a Mg_{Ga} acceptor with nitrogen vacancy (Mg_{Ga}-V_N) complexes showing deep donor–acceptor pair characteristics.[17–19]

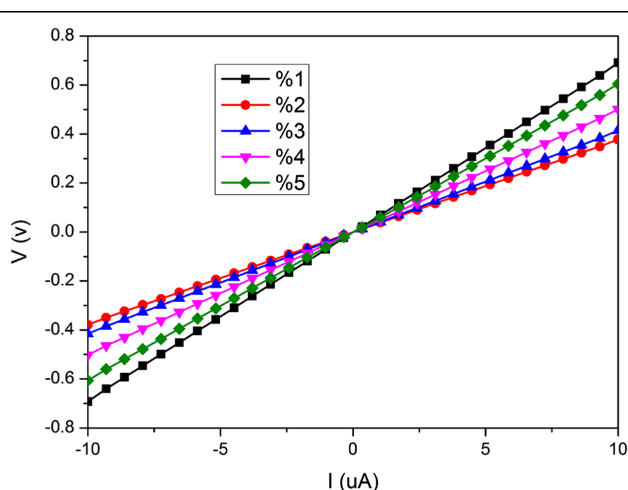

Fig. 2. I–V curves of p-GaN as a function of Cp_2Mg/Ga ratio.

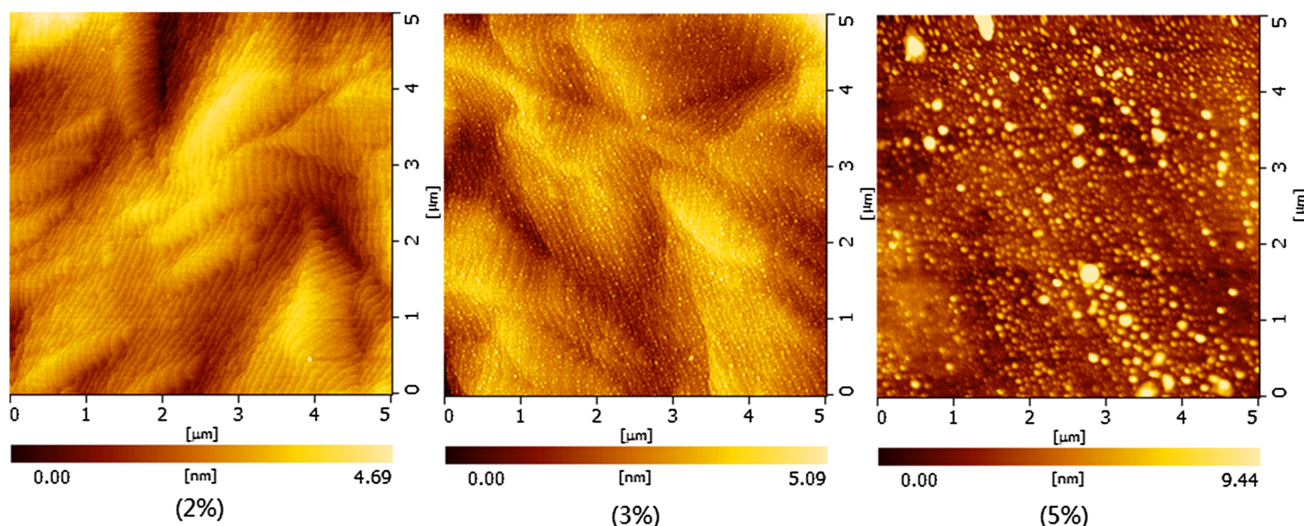

Fig. 3. 5 × 5 μm^2 AFM images of p-GaN with 2%, 3%, and 5% Cp_2Mg/Ga ratio.

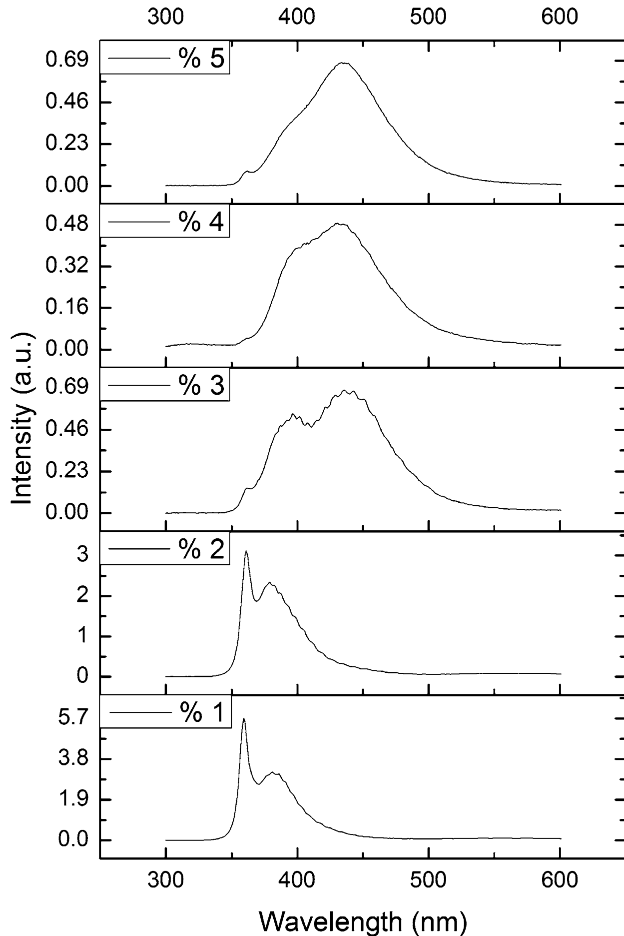

Fig. 4. Room temperature PL spectra of *p*-GaN with different Cp_2Mg/Ga ratios.

The Mg_{Ga}-V_N complexes are in deep donor state and will lead to compensation effects. The energy state model of Mg dopants can been seen in Fig. 5, which exhibits different recombination processes. As shown in Fig. 5, the 385 nm emission corresponding to 3.2 eV originates from a shallow donor to the Mg_{Ga} acceptor recombination and the 440 nm emission corresponding to 2.8 eV originates from deep donor Mg_{Ga}-V_N complexes to Mg_{Ga} acceptor recombination. The amount of deep donors increases as Mg incorporation increases, which indicates that the excess Mg at higher doping level is in the deep donor state. Mg doping at higher concentration is not beneficial to obtain high hole concentration. Through the increase of Mg concentration, the isolated Mg_{Ga} state tends to saturation and Mg_{Ga}-V_N complexes appear and form self-compensation with shallow acceptors. Thus, at higher Mg doping concentration, the hole concentration decreases instead. This result shows good agreement with the electrical characteristics shown in Fig. 1. When 440 nm emission appears, the hole concentration begins to decrease. Combined with the AFM results, the grains at the surface of *p*-GaN may be related to the Mg_{Ga}-V_N complexes and the grain size is determined by the amount of Mg_{Ga}-V_N complexes.

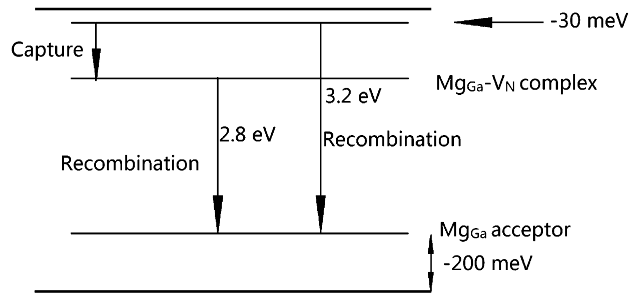

Fig. 5. Energy states and recombination progress in *p*-GaN.

Based on these analyses, the results of Hall measurements shown in Fig. 1 can be explained as follows. With the increase of Cp_2Mg/Ga ratio, the hole concentration first increases and then decreases, and reaches its maximum at 2% Cp_2Mg/Ga ratio. *p*-GaN with 2% Cp_2Mg/Ga ratio has the highest hole concentration, 4.2×10^{17} cm^{-3}. At lower Cp_2Mg/Ga ratio, the increase in hole concentration is attributed to the increase of shallow donors. And at higher Cp_2Mg/Ga ratio, the decrease in hole concentration is due to the self-compensation effect of deep donor state caused by the Mg_{Ga}-V_N complexes formed in *p*-GaN at high Mg doping levels. This would suggest the difficulty in achieving high hole concentration through high Mg doping. AFM and PL measurements are useful tools to analyze whether Mg doping is excess. If grains appear on the surface of *p*-GaN, Mg doping is excess. Larger grain size means a larger degree of excess Mg doping. The appearance of 440 nm emission indicates the formation of Mg_{Ga}-V_N complexes at deep donor state and compensation of shallow acceptor, indicating that the Mg doping is excess.

CONCLUSION

In summary, the influence of Cp_2Mg/Ga ratio in gas phase on the properties of *p*-GaN layers grown by MOCVD has been investigated. *p*-GaN has an optimal doping concentration to obtain high hole concentration when Cp_2Mg/Ga ratio is 2%. Lower Cp_2Mg/Ga ratio leads to less shallow acceptors in *p*-GaN. And at higher Cp_2Mg/Ga ratio, Mg_{Ga}-V_N complexes at deep donor state form and compensate shallow acceptors. Thus, Mg doping has an optimal doping concentration. AFM and PL tests can determine whether the Mg doping is excess. Grains appear on the surface of *p*-GaN in the AFM test, and a 440 nm emission peak appears in the PL test when Mg doping is excess.

ACKNOWLEDGEMENT

This work is supported by the National Natural Science Foundation of China (Nos. 61475110, 61404089 and 21471111), the Open Research Fund of Jiangsu Key Laboratory for Solar Cell Materials

and Technology, Changzhou University (Grant No. 201205), Shanxi Provincial Key Innovative Research Team in Science and Technology (2012041011), the Natural Science Foundation of Shanxi Province (No. 2014021019-1).

REFERENCES

1. A. Krtschil, H. Witte, M. Lisker, J. Christen, U. Birkle, S. Einfeldt, and D. Hommel, *J. Appl. Phys.* 84, 2040 (1998).
2. E. Litwin-Staszewska, T. Suski, R. Piotrzkowski, I. Grzegory, M. Bockowski, J.-L. Robert, L. Konczewicz, D. Wasik, E. Kaminska, D. Cöte, and B. Clerjaud, *J. Appl. Phys.* 89, 7960 (2001).
3. N.D. Nguyen, M. Germain, M. Schmeits, B. Schineller, and M. Heuken, *J. Appl. Phys.* 90, 985 (2001).
4. J.W. Huang, T.F. Kuech, H. Lu, and I. Bhat, *Appl. Phys. Lett.* 68, 2392 (1996).
5. J. Orton and C.T. Foxon, *Rep. Prog. Phys.* 61, 1 (1998).
6. C.G. Van de Walle, C. Stamp, and J. Neugebauer, *J. Cryst. Growth* 189, 505 (1998).
7. U. Kaufmann, M. Kunzer, H. Obloh, M. Maier, Ch. Manz, A. Ramakrishnan, and B. Santic, *Phys. Rev. B* 59, 5561 (1999).
8. U. Kaufmann, P. Schlotter, H. Obloh, K. Köhler, and M. Maier, *Phys. Rev. B* 62, 10867 (2000).
9. H. Alves, M. Böhm, A. Hofstaetter, H. Amano, S. Einfeldt, D. Hommel, D.M. Hofmann, and B.K. Meyer, *Phys. B* 308, 38 (2001).
10. Ch.G.V. de Walle, C. Stampfl, and J. Neugebauer, *J. Cryst. Growth* 189, 505 (1998).
11. Y. Xian, S. Huang, Z. Zheng, B. Fan, Z. Wu, H. Jiang, and G. Wang, *J. Cryst. Growth* 325, 32 (2011).
12. M. Lachab, D.-H. Youn, R.S. Qhalid Fareed, T. Wang, and S. Sakai, *Solid-State Electron.* 44, 16691677 (2000).
13. K.S. Kim, G.M. Yang, and H.J. Lee, *Solid-State Electron.* 43, 1807 (1999).
14. C.-R. Lee, J.-Y. Leem, S.-K. Noh, S.-E. Park, J.-I. Lee, C.-S. Kim, S.-J. Son, and K.-Y. Leem, *J. Cryst. Growth* 193, 300 (1998).
15. U. Kaufmann, M. Kunzer, M. Maier, H. Obloh, A. Ramakrishnan, B. Santic, and P. Schlotter, *Appl. Phys. Lett.* 72, 1326 (1998).
16. U. Kaufmann, M. Kunzer, H. Obloh, M. Maier, Ch. Manz, A. Ramakrishnan, and B. Santic, *Phys. Rev. B* 59, 5561 (1999).
17. M. Smith, G.D. Chen, J.Y. Lin, H.X. Jiang, A. Salvador, B.N. Sverdlov, A. Botchkarev, H. Morkoc, and B. Goldenberg, *Appl. Phys. Lett.* 68, 1883 (1996).
18. M.A. Reshchikov, G.-C. Yi, and B.W. Wessels, *Phys. Rev. B* 59, 13176 (2010).
19. D. Iida, K. Tamura, M. Iwaya, S. Kamiyama, H. Amano, and I. Akasaki, *J. Cryst. Growth* 312, 3131 (2010).